IEEE Robotics & Automation Magazine (RAM) paper, presented at ICRA 2023, London, UK. Cite as RAM paper.

Contact Shape and Pose Recognition: Utilizing Multipole Magnetic Tactile Sensor with Meta-learning Model

Ziwei Xia[1], Bin Fang[2*], Fuchun Sun[2], Huaping Liu[2], Weifeng Xu[3], Ling Fu[3], Yiyong Yang[1*]

***Abstract*—Soft magnetic tactile sensors have been gradually applied to robotic systems due to their low-cost and simple fabrication. The previous soft magnetic tactile sensor was developed for tactile features of a single point (i.e., force/location) estimation and proved the feasibility by experiments. However, extracting tactile features of a surface (i.e., contact shape) by magnetic sensors remains a challenge, which limits the application. In this paper, a soft magnetic tactile sensor that can extract contact surface shape and pose features is fabricated and a multi-pole magnetization method is developed to improve the performance of tactile sensor. Furthermore, we propose a metric-based meta-learning method to extract the tactile feature of the contact surface shape and pose from magnetic data under limited sample conditions and the method is verified by a series of experiments. The experimental results show that our method can achieve more than 80% accuracy in contact shape recognition and more than 95% accuracy in contact pose recognition. The experimental results demonstrate that our method can extract tactile features under limited data conditions and has a certain generalization ability for new contact data.**

***Index Terms*—Soft magnetic sensor, contact shape, magnetism, metric-based meta-learning.**

I. Introduction

As an essential element, robotic tactile sensors have received keen attention and have been shown to greatly enhance the performance of dexterous manipulation for robots [1]. Perception and control for dexterous hands are complementary when grasping and manipulating an object [2]. To date, several types of tactile sensors have been proposed that involve diverse principles, such as piezoresistive sensors [3], capacitive sensors [4]. They have been used in different robotic applications (e.g. force estimation, slip detection, and in-hand manipulation [5]). However, most traditional sensors are commonly not soft enough. Constrained by its principle of sensing, traditional tactile sensors are usually rigid. Therefore, when in contact with an object, only part of the sensor is in contact with the object and it is difficult for these sensors to collect complete tactile information.

[1]Ziwei Xia and Yiyong Yang are with School of Engineering and Technology, China University of Geoscience(Beijing), Beijing, China {xzw, yangyy}@cugb.edu.cn

[2]Bin Fang, Funchun Sun, Huaping Liu are with the Institute for Artificial Intelligence, State Key Lab of Intelligent Technology and Systems, Department of Computer Science and Technology, Beijing National Research Center for Information Science and Technology, Tsinghua University, Beijing, P.R. China. {fangbin, fcsun, hpliu} @tsinghua.edu.cn.

[3]Weifeng Xu and Ling Fu are with Siemens Ltd. , Beijing, China {weifeng.xu, ling.fu}@siemens.com

*correspondence author, fangbin@tsinghua.edu.cn, yangyy@cugb.edu.cn.

A challenging area for robotic tactile sensors is acquiring richer contact information [6]. Therefore, the sensor structure needs to be designed more flexibly to make better contact with the object. Numerous studies have proposed new types of sensors to address this issue [7], [8]. Vision-based tactile sensors adopt an elastomer structure and can perceive continuous contact features [9]. They have been successfully applied to robot manipulation tasks [10]. By simply changing the coating material on the surface, sensors based on the same principle can even detect other modes of information, such as temperature [11]. Magnetic tactile sensors can also be constructed with elastomer and have the same ability to detect continuous contact forces and contact positions [12], [13]. For two important criteria for robot tactile sensors: the resolution and sensing accuracy, magnetic tactile sensors can achieve the desired performance [14]. In addition, a flexible surface means more contact area that can provide better mechanical compliance and surface friction coefficient. Compared to other kinds of tactile sensors previously discussed, soft magnetic tactile sensors or skins are also a potential method for detecting touch and local deformations of soft robotic hand [15], [16].

However, a major challenge with this kind of tactile sensor is the extraction of tactile features. One way to solve this challenge is to optimize the sensor magnetic field distribution. In the early stage, researchers usually used cylindrical magnets and cast silicone elastomer to manufacture magnetic tactile sensor [17]. But magnetic tactile sensors based on this scheme are usually used for detecting contact force information. Gradually, sensor schemes began to evolve into mix permanent particle and elastomer [18]. Compared with the previous scheme, this scheme can obtain more tactile features and contact position information. On the other hand, researchers are also trying to optimize the performance of sensors by changing the distribution of magnetic fields. By combining with the Halbach array, Y. Yan et al. improved the resolution of the magnetic tactile sensor [14]. M. Gui et al. designed a halbach-cylinder-based magnetic skin for tactile sensing [19]. And in this paper, we used multi-pole magnetization method to improve sensor performance. Compared to the Halbach array, the process of our magnetization method is simpler. And compared with the general magnetization method, the sensitivity and signal-to-noise ratio (SNR) of the sensor are improved.

Meanwhile, for this kind of sensor, the neural network (NN) method usually calibrates the sensor. It requires many haptic sample data, such as T. Hellebrekers used $3000 * 100$ samples to calibrate the contact position [12] and Y. Yan who used

IEEE Robotics & Automation Magazine (RAM) paper, presented at ICRA 2023, London, UK. Cite as RAM paper.

90 * 90 * 5 sets of data to realize a tactile super-resolution model [20]. For a new object, the result of sensor output will produce a large error. To solve this limitation, we combined metric-based meta-learning to process sensor data. It can reduce the amount of required data at the state of extracting tactile features. It also allows sensors to extract tactile features based on previous tactile data. We verified that this method can recognize the shape and position features of the new contact object based on the existing tactile features. It is useful to extract the contact features from tactile data. For example, the shape features of the contact surface are used for slip detection and in-hand manipulation tasks [21], [22], and the texture features are essential to material recognition tasks [23]. Therefore, we attempt to extract the tactile feature of the contact object from raw tactile information based on existing data.

To sum up, the presented magnetic tactile sensor includes the following contributions:

1) A new multi-pole magnetization method is used to optimize the performance of magnetic tactile sensors.
2) Combined with the meta-learning method, the data collected by the magnetic tactile sensor are processed. It allows the tactile sensor to use previous knowledge of contact features to predict the contact state of the same type of object. It reduces the time required to collect data when using sensors.
3) The effectiveness of the sensor and the generalization ability of the proposed model are verified by a series of experiments. The sensor has the ability to classify different contact shapes and poses.

The remainder of this paper is structured as follows. In section II, we describe the design and fabrication of our magnetic sensor system. Section III discusses the aspects of magnetization that are used in our sensor surface and compares their performance and then selects the best scheme. Section IV introduces the method our sensor used to extract tactile features. Section V describes the process of data collection and a series of experiments to verify the performance of sensors and algorithms. Finally, we summarize and prospect our work.

II. Materials

A. Sensor Design

Fig. 1 shows the configuration of the proposed magnetic tactile sensor. The sensor consists of four parts: a magnetic layer, silicone layer, pedestal, and 3D Hall effect sensor array. The components of the magnetic layer are permanent magnetic particles (LW-Q-100 (the particle size is 100 meshes), manufactured by Xinnuode company) and silicone rubber (Ecoflex 0030, manufactured by Smooth-on, Inc.). The silicone layer is made of the same silicone material as the magnetic layer which is between the magnetic layer and pedestal to increase the deformation of the magnetic layer when in contact with an object. The pedestal is used to hold the Hall effect sensor and silicone layer and the sensor array is used to measure the change in the magnetic field. We select five locations to measure the magnetic field values. The five locations are uniformly distributed on the sensor surface to detect the changes in the magnetic field of the entire magnetic layer. We place an array of four 3D Hall effect sensors (MLX90393, manufactured by Melexis, Inc.) at each measurement position.

The principle of this sensor is as follows: first, the magnetic layer produces deformation when the magnetic sensor is in contact with an object, which will result in the displacement of permanent magnetic particles in the magnetic layer. The changed magnetic field values can be collected by five Hall effect sensor arrays. We extract the tactile features by analyzing the collected data.

B. Fabrication

In the fabrication process, liquid silicone rubber and permanent magnetic particles are mixed at a weight ratio of 1:1 to form a magnetic layer, during which time the materials are not magnetic. Then we pull it into an $75mm*75mm*2mm$ mold, and the mold and liquid silicone rubber with the magnetic particle are put into a vacuum machine for curing. After it solidifies, we magnetize it by putting it in a magnetizing machine. After magnetization, permanent magnet materials in the magnetic layer can retain magnetism to provide magnetic field information. Meanwhile, we pull liquid silicone into the sensor pedestal to form a silicone layer. After the silicone layer is solidified, we coated the bottom of the magnetic layer with the same liquid silicone and then pressed it against the silicone layer. When the liquid silicone between the two layers solidifies, the magnetic layer, silicone layer, and pedestal are bonded to form a complete elastomer. Finally, we mounted the sensor array at the bottom of the sensor pedestal to complete the overall assembly of the magnetic tactile sensor. The overall size of the magnetic sensor is $80mm * 80mm * 7mm$, the thickness of the magnetic layer, silicone layer and Hall effect sensor is 2mm and the thickness of the pedestal is 1mm.

For the Hall effect sensor array, we cascade multiple Hall effect sensors to form a bus acquisition network. By using an IIC (Inter-Integrated Circuit) bus, the acquisition frequency of the Hall effect sensor is better than 80 Hz to ensure the sensor array responds quickly to the change in the magnetic field. The

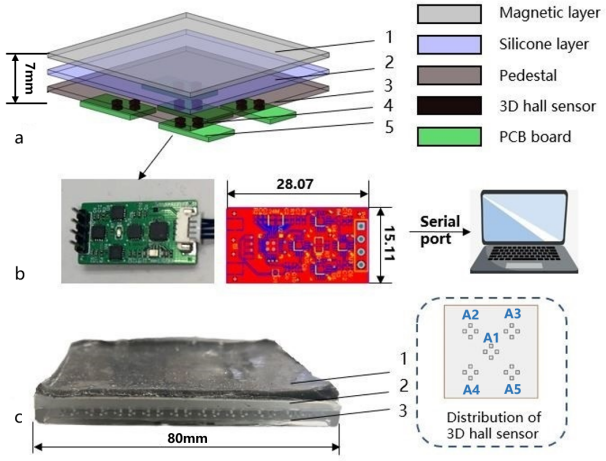

Fig. 1. Illustration of the sensor structure. a) The designed pattern. a) The 3D Hall effect sensor array and its communication protocol. c) Prototype of the magnetic elastomer part and the distribution of the Hall effect sensor.

sensor array can acquire the magnetic field intensity of twenty points shown in Fig. 1.

III. Magnetic Field for Sensor

For the proposed magnetic tactile sensor, the distribution of the surface magnetic field will affect its performance. As long as the magnetic layers are magnetized in different postures, they can generate different magnetic fields. To improve the performance of the proposed sensor, we consider changing the posture of the magnetic layer when it is magnetized to obtain the effect of multipole magnetization. We compare the performance of the multipole magnetization and the commonly used magnetization method.

A. Magnetization

The residual flux strength of a soft magnetic layer is usually not as good as that of a hard magnet under the same magnetization conditions. However, to ensure that the sensor can receive a stable magnetic field signal, it is necessary to make the residual flux strength of the magnetic layer sufficiently large. In the process of magnetization, the magnetic direction, and the shape of the magnetic layer affect the distribution of the remaining magnetic field. It is expected that by changing the magnetization method, the characteristics of the magnetic layer can improve.

Halbach magnetization methods and folding magnetization methods have shown unique advantages in improving magnetic tactile sensor performance [14], [24]. The folding magnetization method allows for a higher magnetic flux at a particular location. To improve the performance of the magnetic tactile sensor, we enhance the magnetic flux above the Hall effect sensor array to acquire a higher quality magnetic signal. Therefore, we used multi-pole magnetization method to magnetize the magnetic layer and it is able to form a multi-pole magnetic field in its surface. For the magnetic field formed by using this magnetization method, we have carried out simulation analysis and actual measurement respectively. The result is shown in fig. 2.

B. Test

First, we measure the magnetic field distribution of the magnetic layer. As shown in Fig. 2, the actual magnetic field strength distribution for multipole magnetic layer is similar to the simulation results. Above the location of the Hall effect sensor array, the magnetic field strength is relatively large. Next, the advantages of this magnetization method are illustrated by experiments.

First, we build a data acquisition platform. The data acquisition platform is shown in Fig.3. The measuring head is fixed on a four-axis mobile platform. When collecting data, the sensor is fixed above the platform. By adjusting the four-axis moving platform, we can load force at different positions of the sensor. We test the four different magnetization surfaces by using a tapered measuring head to press them with the same velocity and location. We collect magnetic field values in the loading progress for analysis.

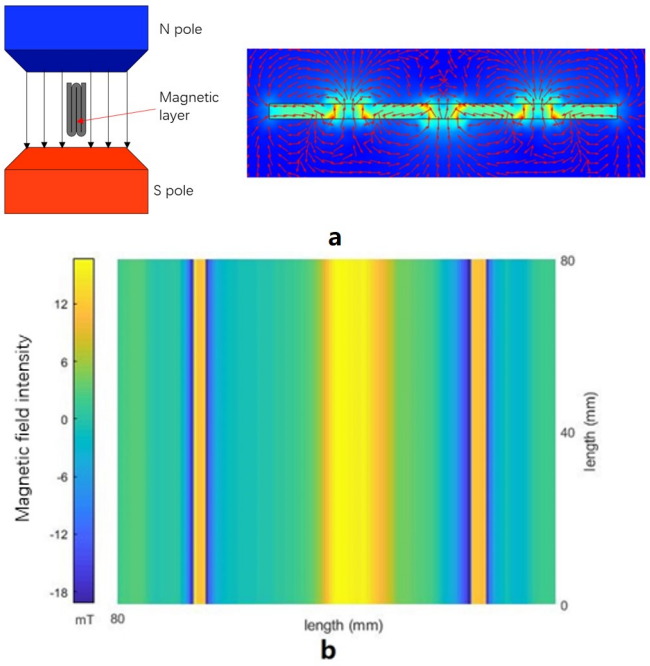

Fig. 2. Diagram of the magnetic field distribution. a) Multi-pole magnetization methods and the simulation result of the distribution of magnetic field. b) Actual measured magnetic field strength in the z direction of multi-pole magnetization method.

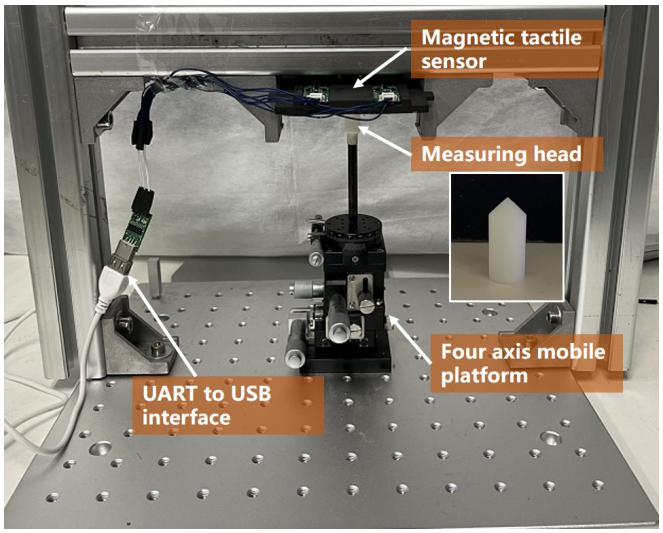

Fig. 3. The data acquisition platform. The four axis mobile platform is used to adjust the measuring head. The UART to USB interface is used to transmit Hall effect sensor data to the computer.

The SNR is an important indicator for the sensor. For the proposed sensor, we define the SNR as:

$$SNR = 20 * log_{10}(\frac{|m - m_0|}{\sigma})dB \tag{1}$$

where m_0 is the output of the sensor in the non-contact state, and m is the output of the sensor in the contact state. σ is the standard deviation when not loaded.

The results are shown in Fig. 4. For the same position, a higher magnetic field will lead to a better SNR. Therefore, by utilizing the multi-pole magnetic layer, the collected magnetic

field information contains more contact features than other magnetic surfaces. When the sensor contacts the object, the response is also obvious. It is conducive to processing the raw data for tactile recognition. In the next section, we introduce the details of our method for contact surface and pose recognition.

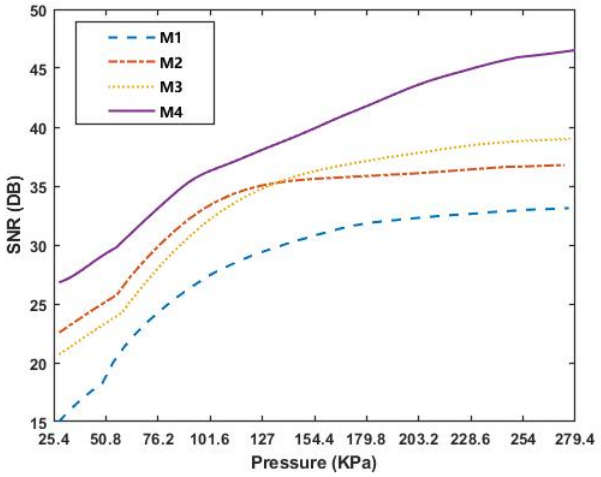

Fig. 4. The SNRs of four tactile sensors with different magnetic fields. Curves 1, 2, 3, 4 corresponding to four magnetization methods (Magnetization method 1 (M1): Magnetize along the Z direction. b) Magnetization method 2 (M2): Magnetize along the Y direction. Magnetization method 3 (M3): Fold the magnetic surface in half and magnetize along the Y direction. d) Magnetization method 4 (M4): Magnetize along the Y direction. Fold the magnetic film three times and magnetize along the Y direction.) respectively. Loading position: Directly above sensor array A1.

In addition, we tested the actual response of the sensor using the same experimental platform. The experimental results are shown in Fig.5. The test results show that the multi-pole magnetic layer tactile sensor shows a greater variation of the magnetic strength. It means that the sensors are more sensitive in measuring contact with objects.

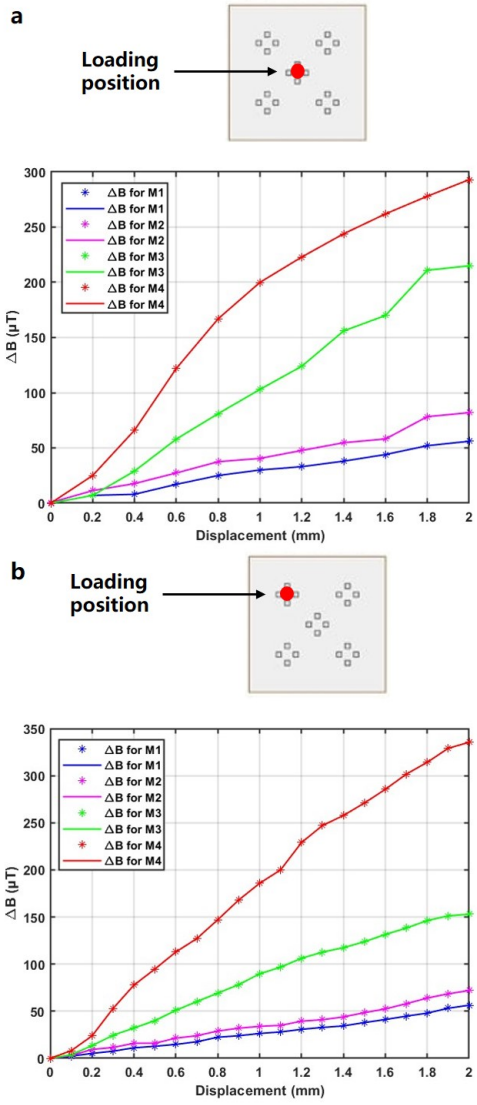

Fig. 5. Results of the change in magnetic strength when in contact with measuring head. a) Actual result measured by sensor array A1. b) Actual result measured by sensor array A2. Δ B is the total magnetic field change value measured by the sensor array. The magnetic field distribution on the surface of sensor arrays A2 to A5 is similar, so the experimental results are similar, and only the result of A2 is shown.

IV. METHOD

When objects contact the magnetic tactile sensor, the collected magnetic data include the shape and pose information of the contact surface. The existing magnetic tactile sensor process methods usually direct contact position and force recognition through combination with deep neural network (DNN) methods and obtain good results [14]. However, related works are few for contact surface shape and pose recognition using magnetic tactile sensors. To calibrate the sensor, the DNN methods always need many labeled samples (e.g., in [14], they used 40500 samples to train DNN model to achieve the calibration of only an object). In practice, this approach is a limitation for the popularization of the use of magnetic tactile sensors. In this part, we introduce the contact surface recognition method which uses prototypical networks (Pronet) based on limited samples and obtains good results.

A. Few-shot meta-learning

It is easy for humans to learn to recognize a new object from a few instances because the human can use prior knowledge to learn. Inspired by this ability, the meta-learning method, a flexible framework that can learn prior knowledge from performing related tasks is presented. At present, there are two main kinds of meta-learning method: metric-based meta-learning (e.g. matching network [25], siamese network [26] and prototypical network [27]) and optimization-based meta-learning (e.g. Model-Agnostic Meta-Learning (MAML) [28]). Based on meta-learning method, researchers have solved some problems: few-shot fault diagnosis [29], image classification [27] and speech recognition [30]. For this paper, combined with metric-based meta-learning methods (Pronet), we extract and recognize the contact features based only on magnetic field information.

B. Problem definition

For few-shot shape and contact status classification, we define this problem following reference [27]. We organize the few-show tactile recognition tasks according to the N-way K-shot protocol. In the process of meta-training, the training set contains a labeled few-shot support set $D_{TS} = \{(x_1^n, y_1^n), ..., (x_i^n, y_i^n)\}$ equals to $N \times K$ (K is usually a small value, such as 1 or 5)and unlabeled query set $D_{TQ} = \{(x_1^q, y_1^q), ..., (x_i^q, y_i^q)\}$ equals to $N \times M$ (M can be any value). Among these, N represents the categories of samples, K and M represents the number of samples for each type. For our problem, each sample in the support set consists of input data $x \in R^{D \times L}$ to vibration magnetic signal of length L for each magnetic feature and the label $y \in \{1, 2, 3, ..., N\}$ means the shape of object or contact status. For the training stage, we sample a series of tasks $T^t = \{D_{TS}^N, D_{TQ}^N\}$ to train the model. The purpose of this model is to correctly classify N types of D_{TQ} based on the D_{TS}.

C. Architecture of the metric-based meta-learning model

The flow chart of our model for contact surface recognition is shown in Fig. 6. The overall process of the algorithm is similar to that of Pronet. First, we collected raw magnetic contact information of multiple objects in different locations. Then we buily the training set, testing set, and valid set based on these data. Through feature extraction, D_{TS} and D_{TQ} are both converted to feature maps. Finally, we calculate the prototypical features of each category, and calculate the distance between the feature of query set and prototypical features to predict the classification of new data.

In the feature extraction stage, each x in D_{TQ} is converted to a P-dimension vector in feature space by CNN (Convolutional neural network): $(f_\theta(x_i^n) : x_i^n \rightarrow \mathbb{R}^P)$, where θ is the learnable parameter of CNN. Then we calculate the prototype for these N classes

$$p_n = \frac{1}{K} \sum_{(x_i^n, y_i^n) \in D_{TS}} f_\theta(x_i^n) \tag{2}$$

where K is the set of examples labeled with class k. Then $d = d(f_\theta(x_i^q), p_n)$ which is the distance between x_q^n (samples in D_{TQ}) and the prototype p_n, is calculated. For this model, we choose squared Euclidean distance to metric the distance. Considering that the distance represents the similarity, we define the probability of the sample to it class N based on prototype as follows:

$$p(y = n|p_n) = \frac{exp(d(f_\theta(x_i^q), p_n))}{\Sigma_{m=1}^N exp(d(f_\theta(x_i^q), p_m))} \tag{3}$$

To minimize the distance in the feature space between the sample and the corresponding prototype, the purpose of the network is to minimize the cross-entropy loss, which is defined as:

$$Loss_1 = -logp(y = n|p_n) \tag{4}$$

Then we also expert maximized the distance between each different class of samples. When we calculate the prototype for each category k, we calculate the Euclidean distances between the category prototypes and normalize them. Therefore we define loss function 2 as:

$$Loss_2 = \Sigma_{i=1,j=1,i \neq j}^N \frac{1}{(1 + D(p_i, p_j))} \tag{5}$$

p_i and p_j are the prototypes of two different categories. $D(.)$ represents calculating the Euclidean distance between two prototypes p_i and p_j. The total loss function is defined as:

$$Loss_{total} = Loss_1 + \alpha \times Loss_2 \tag{6}$$

where α is a hyper-parameter, in this paper we choose 0.1. In the process of meta training, the purpose is to minimize the loss and optimize the parameters in the feature extraction model.

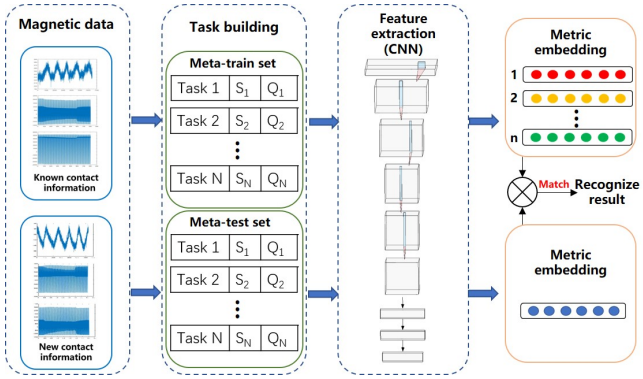

Fig. 6. The flow chart of our method.

In the experimental part, we compare the performance of Pronet with the optimized loss function (Pronet-L) and the original Pronet.

D. Model details

In this work, a simple end-to-end feature extraction network is proposed. The input of this CNN model is a size of 60 (magnetic field intensity value from 20 sensors in the x, y, and z directions) $\times$ 10 (time step) magnetic signals. The details of the CNN are shown in Table. I. The network has three convolutional layers and maxpool layers. The batch-norm layer is used to standardize raw data. In the end, the network generates a feature vector for each sample. In addition, the other details (hyper-parameter, meta-learning setting) used for meta-training of our model are shown in Table. II.

E. Performance evaluation

In the stage of performance evaluation, we put all the support sets used for meta-valid into the trained model. Then the prototype of each class was computed and all the unlabeled samples from the meta-valid set were also similarly used to compute the feature. By measuring the distance between the prototype of support set and the features of unlabeled samples, we can obtain the contact surface shape and contact pose classification results.

TABLE I
DETAILS OF CNN NETWORK.

Layer	Kernel size	Channels (in, out)	Stride	Padding
Conv2D 1	(2,2)	(1,16)	(2,2)	Yes
Batchnorm2D 1				
ReLU 1				
MaxPool2d 1	(2,1)	(16,16)	(2,1)	No
Conv2D 2	(2,2)	(16,32)	(2,2)	Yes
ReLU 2				
MaxPool2d 2	(2,1)	(32,32)	(2,1)	No
Conv2D 3	(2,2)	(32,64)	(2,1)	Yes
ReLU 3				
MaxPool2d 3	(2,1)	(64,64)	(2,1)	No

TABLE II
DETAILS OF THE MODEL SETUP.

Description	Value
Optimizer	Adam
Learning rate	0.0001
Batch size	32
Maximum epochs	100
Distance metric	Squared Euclidean distance
Tasks per epoch	100
Support samples per class (K_s)	1,3,5
Query samples per class (K_q)	10-K_s

V. EXPERIMENTS

For this part, the details of the experimental setup are described and the tactile feature extraction method is evaluated by a series of experiments. The process of data collection and the method used for object shape and contact mode are all elaborated. We also show and discuss the experimental results in the end.

A. Experimental setup and data collection

The experimental device is a Z-axis movement platform and a digital force gauge. A series of resin measuring heads with different shapes were designed for collecting contact shape information. The sensor is fixed on the platform and loaded by the measuring head which is attached to a digital force gauge in the process of data collection. In Fig. 7 and Fig. 8, we show some of the measuring heads. For the contact surface shape and pose feature classification, we use three different shapes (square, triangle, and circle) of the measuring head (a-c in Fig. 7) to collect shape information and three bar-type measuring heads to collect six different contact pose information.

In the process of contact surface shape classification data collection, we select 25 evenly distributed points on the tactile sensor as shown in Fig 7. For each contact point, we collected 30 samples for each measuring head at 20 Hz. The raw magnetic data were recorded, and then we manually labeled these data. For contact status data collection, the overall process is similar. The only difference is that we need to collect contact mode information for each of the 25 points in six postures which are shown in Fig. 8 by using measuring heads 1 - 3.

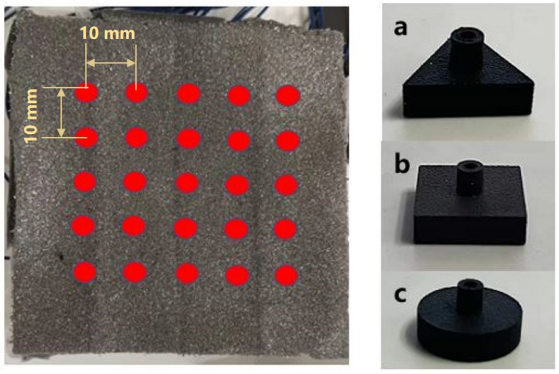

Fig. 7. Contact location of the magnetic tactile sensor in the process of data collection and measuring head which has different shape features.

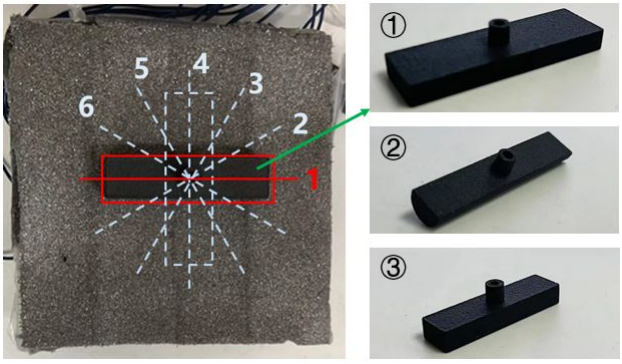

Fig. 8. The six contact status we define and three measuring heads used for data collection.

B. Experiment I: Contact surface's shape classification

For tactile sensors of the same magnetic-based principle, researchers have used it for measuring contact force and position [14]. Usually, they used the deep learning method to train a model that can establish the relationship between raw magnetic data and contact position. A traditional supervised learning method for contact surface shape recognition usually needs to prepare a large amount of labeled data to train the model. When the sensor is used for measuring other types of contact objects, researchers need to re-collect a large amount of labeled data on this kind of object. However, there may be only a few data samples of a new shape when the sensor contacts a new object in the actual environment. Therefore it limits the use and spread of magnetic tactile sensors.

The raw magnetic data include both the contact surface shape and pose feature besides location and force feature. For an identical object, when it contacts the tactile sensor at different locations, the response magnetic signal is different. Therefore it is difficult to collect the contact information of an object at each location of the magnetic sensor for contact surface shape recognition, and it is time-consuming to collect

many actual contact samples of a new object. Therefore, in this paper, we utilize a metric-based meta-learning method for solving the few-shot contact surface shape and pose feature recognition problem. The purpose of our method is to identify contact features based on a few samples.

In the experimental state, the dataset of contact surface shape recognition is collected from the magnetic tactile sensor under different measuring head load conditions at 25 positions which are shown in Fig. 7. There are four different shapes of measuring heads: triangle, square, circle, and rectangle. The first three shapes include three different sizes: 10mm, 15mm, 20mm. Each measuring head has 750 contact samples and each sample is 3 dimensional magnetic signal with 20 points.

We set 80% of the collected data as a meta-training set and the other 20% for which contact at other locations is set as a meta-testing set. Based on the few-shot learning setup, for 5-way 1-shot contact surface shape recognition, we take 10 samples from each category, one of the samples in each category is used for the support set, nine other samples are used as query set. The setting for 5-way 3-shot and 5-way 5-shot is similar to this.

We use a Pronet model and improved Pronet-L to assess the performance for contact surface shape recognition. In addition to few-shot learning methods, we also use two other methods for comparison respectively: machine learning method (kNN, k-Nearest Neighbor) and deep learning method (CNN). The contact shape classification accuracy results in meta-testing process are given in Table. III. Accuracy is defined by the number of correct classifications divided by the number of all samples in query set. To compare these models, the results we present show better performance than each other model on the same contact surface shape recognition dataset. All experiments are implemented on the computer with one Nvidia GeForce RTX 2060 GPU and one Intel Core i7-9700F CPU.

TABLE III
FEW-SHOT SHAPE CLASSIFICATION ACCURACY OF DIFFERENT METHODS.

Model	Accuracy(%)
Pronet(1-shot)	78.26
Pronet-L(1-shot)	81.33
Pronet(3-shot)	79.18
Pronet-L(3-shot)	84.18
Pronet(5-shot)	80.31
Pronet-L(5-shot)	84.60
KNN (K-NearestNeighbor)	34.59
CNN	26.76

The experimental results show that the Pronet-L is better than the Pronet model in terms of recognition accuracy. The kNN method and CNN method show poor performance in the contact surface shape recognition. Because the tactile feature in the raw magnetic data is complicated includes force feature, contact mode feature, location feature, and shape feature. It is difficult to extract the contact surface shape feature by kNN or CNN methods. The former has limited ability to extract features, while the latter requires more datasets. However in the case of limited data, the Pronet model can also obtain the ability of shape feature extraction better than the kNN and CNN methods.

TABLE IV
FEW-SHOT ORIENTATION RECOGNITION OF TACTILE DATASET.

Different contact orientations	
Meta-training set	Meta-testing set
Measuring head 1 and 2	Measuring head 3
Measuring head 1 and 3	Measuring head 2
Measuring head 2 and 3	Measuring head 1

In addition, we used five new measuring heads (rectangle: $10mm \times 15mm$ and $8mm \times 12mm$, circle: diameter $12mm$, square: $12mm$ side, and triangle: $12mm$ side) to collect data for meta-valid. In the meta-valid process, we split the newly collected data into support sets and query sets. Then the support sets are put into the trained model to calculate the corresponding prototype. The classification is obtained by calculating the distance between the data in the query set and the prototype. The classification accuracy of the best model (Pronet-L) can still be maintained at $82.88\% \pm 2.1\%$. It shows that the model has the ability to extract new contact surface shape features.

C. Experiment II: Contact poses classification

The pose of objects relative to the tactile sensor is an important feature for robotic hands to perform manipulation. For example, to achieve the peg-in-hole task, the robotic hand should know the attitude of the peg relative finger. However, the manipulated object is always changed in actual manipulation tasks. Therefore, the contact pose recognition model should have the ability to adapt to different manipulated objects.

For our experiments, we define six contact poses between the bar-type measuring head and tactile sensor as shown in Fig. 7. A. We list the few-shot contact mode classification of our dataset under the different measuring head conditions which have six contact poses in Table. IV.

For contact status classification, we analyze three scenarios: 1-shot, 3-shot, and 5-shot learning between different measuring head conditions. The results are shown in Table. V. All of these methods perform well on these tasks but are still not as accurate as the 1-shot learning methods. These results indicate that the features of the contact pose under different measuring head conditions are similar. However, the metric-based meta-learning method can achieve the best performance in a 5-shot learning setting. Pronet-L has the best performance for addressing this issue, and the optimized loss function can improve the performance of the model.

We randomly select the contact points on the tactile sensor beside the 25 points shown in Fig. 7 to collect some unlabeled samples. All these samples are used for meta-testing. The results are shown in Fig. 9. Even under the condition that the measuring heads are in contact with tactile sensors at other positions, the few-shot learning methods still guarantee good recognition accuracy. The other two methods perform worse than the state of meta-valid (reduce approximately 10%

TABLE V
FEW-SHOT CONTACT STATUS CLASSIFICATION OF TACTILE DATASET.

accuracy(%)			
	Measuring head 1 and 2 → 3	Measuring head 1 and 3 → 2	Measuring head 2 and 3 → 1
Pronet(1-shot)	91.25	91.86	91.78
Pronet-L(1-shot)	92.23	92.14	93.07
Pronet(3-shot)	94.64	95.12	94.76
Pronet-L(3-shot)	95.78	95.34	95.14
Pronet(5-shot)	97.88	98.14	98.28
Pronet-L(5-shot)	98.44	98.26	98.45
KNN (K-NearestNeighbor)	92.85	93.54	93.07
CNN	89.15	87.58	90.47

accuracy). This finding suggests that few-shot learning used for contact pose recognition has better generalization ability compared with the other two methods.

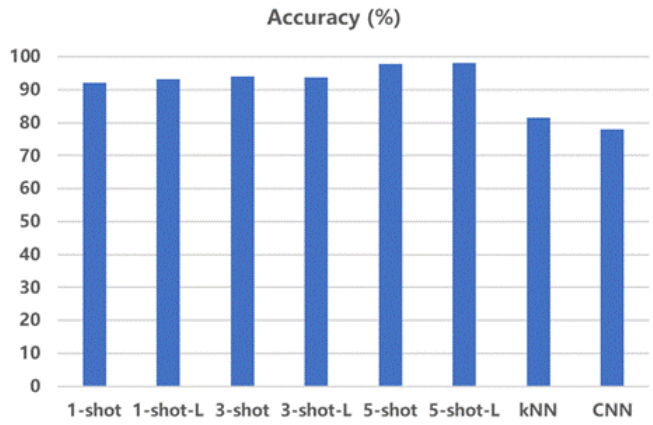

Fig. 9. The results of unlabeled sample classification.

D. Discussion

The core task of few-shot tactile feature recognition is effectively extracting and representing features from magnetic data. Based on the few-shot contact information with the label, the proposed model considers both the similarity between prototype and sample and the similarity between each prototype, which is useful to extract tactile features. For these two tasks, the proposed method achieves more than 80 recognition accuracy. The effectiveness of the proposed method is verified by experiments. In addition, it is worth noting that the recognition accuracy of contact pose is higher than the recognition accuracy of contact surface shape. This is because the measuring head used for contact surface shape recognition is usually smaller than the measuring head used for contact pose recognition. In the contact state, the magnetic strength changes caused by smaller measuring heads can only be detected by fewer Hall effect sensors. As a result, the contact data generated for smaller measuring heads contain fewer tactile features. Therefore, there is still a certain gap between the recognition accuracy of the two tasks.

Another advantage of the approach used in this article is that it requires less contact data. At the same time, this method makes the sensor have a certain generalization. Compared with the machine learning method and deep learning method, the metric-based method is more efficient. The metric-based meta-learning method has the potential to be used for tactile feature extraction.

VI. CONCLUSION

In this paper, a novel magnetic tactile sensor based on the multi-pole magnetization method is designed for extracting contact surface features. The proposed magnetization method offers the advantages of higher SNR and sensitivity which achieve better performance in tactile feature extraction. Meanwhile, we proposed a method combined with meta-learning that enhances the perception ability and generalization of the sensor. Two experiments are designed to simulate different contact shapes and poses, and the experimental results show that the presented metric-based meta-learning method has better classification and generalization performance compared with deep learning methods. The Pronet-L model works by utilizing the prior knowledge learned from previous contact data to achieve new contact shape and pose classification, and the accuracy of the classification results reached 80% and 95%, respectively.

Although the proposed method could enhance the ability of tactile feature extraction for a magnetic tactile sensor, it still remains a challenge to perform complex tactile recognition tasks (e.g., 3D object reconstruction from tactile features). Therefore, it is necessary to research on a better tactile feature extraction framework based on soft magnetic tactile sensor. In addition, the structure of the sensor still has room for improvement include adjusting the distribution of Hall effect sensor array and the number of sensors. In the future work, we will further investigate on these two aspects.

In conclusion, we introduce the process of magnetic tactile sensor fabrication first in this research. By optimizing the magnetization for the magnetic layer, the performance of this sensor is improved. Especially in terms of the SNR, we collect the magnetic field variation in the same location. Under the same loading conditions, an optimized magnetic surface can obtain higher quality tactile signals. In addition, by using the metric-based meta-learning method, the tactile sensor can

extract tactile surface features from a few amounts of data. A series of experiments are carried out to verify the feasibility of the Pronet-L model.

In future work, we would like to further optimize the design scheme including the magnetization mode and structure, and extend our method to extract more tactile features. We would also like to combine our magnetic tactile sensor with dexterous hands to perform complex manipulation tasks.

ACKNOWLEDGMENT

This work is supported by National Key Research Program of China with Project No.2019YFB1309803 and Tsinghua University (Department of Computer Science and Technology)-Siemens Ltd., China Joint Research Center for Industrial Intelligence and Internet of Things.

REFERENCES

[1] J. Tegin and J. Wikander, "Tactile sensing in intelligent robotic manipulation - A review," *Industrial Robot*, vol. 32, no. 1, pp. 64–70, 2005.

[2] M. Bianchi, J. Bohg, H. Moon, R. Platt, and R. Walker, "Robotic hands, grasping, and manipulation [tc spotlight]," *IEEE Robotics Automation Magazine*, vol. 28, no. 2, pp. 131–133, 2021.

[3] Y. Zhang, Y. Mukaibo, and T. Maeno, "A multi-purpose tactile sensor inspired by human finger for texture and tissue stiffness detection," in *2006 IEEE International Conference on Robotics and Biomimetics*, 2006, pp. 159–164.

[4] F. Castelli, "An integrated tactile-thermal robot sensor with capacitive tactile array," *IEEE Transactions on Industry Applications*, vol. 38, no. 1, pp. 85–90, 2002.

[5] A. Billard and D. Kragic, "Trends and challenges in robot manipulation," *Science*, vol. 364, no. 6446, 2019.

[6] H. Yousef, M. Boukallel, and K. Althoefer, "Tactile sensing for dexterous in-hand manipulation in robotics - A review," *Sensors and Actuators, A: Physical*, vol. 167, no. 2, pp. 171–187, 2011. [Online]. Available: http://dx.doi.org/10.1016/j.sna.2011.02.038

[7] N. F. Lepora and J. Lloyd, "Optimal deep learning for robot touch: Training accurate pose models of 3d surfaces and edges," *IEEE Robotics Automation Magazine*, vol. 27, no. 2, pp. 66–77, 2020.

[8] K. Hoshino and D. Mori, "Three-dimensional tactile sensor with thin and soft elastic body," in *2008 IEEE Workshop on Advanced robotics and Its Social Impacts*, 2008, pp. 1–6.

[9] W. Yuan, S. Dong, and E. H. Adelson, "GelSight: High-resolution robot tactile sensors for estimating geometry and force," *Sensors (Switzerland)*, vol. 17, no. 12, 2017.

[10] E. Donlon, S. Dong, M. Liu, J. Li, E. Adelson, and A. Rodriguez, "Gelslim: A high-resolution, compact, robust, and calibrated tactile-sensing finger," in *2018 IEEE/RSJ International Conference on Intelligent Robots and Systems (IROS)*, 2018, pp. 1927–1934.

[11] B. Fang, H. Xue, F. Sun, Y. Yang, and R. Zhu, "A cross-modal tactile sensor design for measuring robotic grasping forces," *Industrial Robot*, vol. 46, no. 3, pp. 337–344, 2019.

[12] T. Hellebrekers, N. Chang, K. Chin, M. J. Ford, O. Kroemer, and C. Majidi, "Soft Magnetic Tactile Skin for Continuous Force and Location Estimation Using Neural Networks," *IEEE Robotics and Automation Letters*, vol. 5, no. 3, pp. 3892–3898, 2020.

[13] R. Bhirangi, T. Hellebrekers, C. Majidi, and A. Gupta, "Reskin:versatile, replaceable, lasting tactile skins," in *CoRL*, 2021.

[14] Y. Yan, Z. Hu, Z. Yang, W. Yuan, C. Song, J. Pan, and Y. Shen, "Soft magnetic skin for super-resolution tactile sensing with force self-decoupling," *Science Robotics*, vol. 6, no. 51, p. eabc8801, 2021.

[15] A. Mohammadi, Y. Xu, Y. Tan, P. Choong, and D. Oetomo, "Magnetic-based soft tactile sensors with deformable continuous force transfer medium for resolving contact locations in robotic grasping and manipulation," *Sensors (Switzerland)*, vol. 19, no. 22, pp. 1–14, 2019.

[16] N. Bira, P. Dhagat, and J. R. Davidson, "A review of magnetic elastomers and their role in soft robotics," *Frontiers in Robotics and AI*, vol. 7, 2020. [Online]. Available: https://www.frontiersin.org/article/10.3389/frobt.2020.588391

[17] H. Wang, G. De Boer, J. Kow, A. Alazmani, M. Ghajari, R. Hewson, and P. Culmer, "Design methodology for magnetic field-based soft tri-axis tactile sensors," *Sensors*, vol. 16, no. 9, 2016. [Online]. Available: https://www.mdpi.com/1424-8220/16/9/1356

[18] T. Hellebrekers, O. Kroemer, and C. Majidi, "Soft magnetic skin for continuous deformation sensing," *Advanced Intelligent Systems*, vol. 1, no. 4, p. 1900025, 2019. [Online]. Available: https://onlinelibrary.wiley.com/doi/abs/10.1002/aisy.201900025

[19] M.-J. Gui, X.-H. Zhou, X.-L. Xie, S.-Q. Liu, H. Li, T.-Y. Xiang, J.-L. Wang, and Z.-G. Hou, "Design and experiments of a novel halbach-cylinder-based magnetic skin: A preliminary study," *IEEE Transactions on Instrumentation and Measurement*, vol. 71, pp. 1–11, 2022.

[20] Y. Yan, Y. Shen, C. Song, and J. Pan, "Tactile super-resolution model for soft magnetic skin," *IEEE Robotics and Automation Letters*, vol. 7, no. 2, pp. 2589–2596, 2022.

[21] B. Romero, F. Veiga, and E. Adelson, "Soft, round, high resolution tactile fingertip sensors for dexterous robotic manipulation," in *2020 IEEE International Conference on Robotics and Automation (ICRA)*, 2020, pp. 4796–4802.

[22] S. Dong, W. Yuan, and E. H. Adelson, "Improved gelsight tactile sensor for measuring geometry and slip," in *2017 IEEE/RSJ International Conference on Intelligent Robots and Systems (IROS)*, 2017, pp. 137–144.

[23] W. Zheng, B. Wang, H. Liu, X. Wang, Y. Li, and C. Zhang, "Bio-inspired magnetostrictive tactile sensor for surface material recognition," *IEEE Transactions on Magnetics*, vol. 55, no. 7, pp. 1–7, 2019.

[24] X. Zhang, H. Hu, D. Tang, C. Zhang, J. Fu, and P. Zhao, "Magnetic flexible tactile sensor via direct ink writing," *Sensors and Actuators, A: Physical*, vol. 327, p. 112753, 2021. [Online]. Available: https://doi.org/10.1016/j.sna.2021.112753

[25] O. Vinyals, C. Blundell, T. Lillicrap, K. Kavukcuoglu, and D. Wierstra, "Matching networks for one shot learning," *Advances in Neural Information Processing Systems*, no. Nips, pp. 3637–3645, 2016.

[26] L. Bertinetto, J. Valmadre, J. F. Henriques, A. Vedaldi, and P. H. S. Torr, "Fully-convolutional siamese networks for object tracking," in *Computer Vision – ECCV 2016 Workshops*, G. Hua and H. Jégou, Eds. Cham: Springer International Publishing, 2016, pp. 850–865.

[27] J. Snell, K. Swersky, and R. Zemel, "Prototypical networks for few-shot learning," *Advances in Neural Information Processing Systems*, vol. 2017-Decem, pp. 4078–4088, 2017.

[28] C. Finn, P. Abbeel, and S. Levine, "Model-agnostic meta-learning for fast adaptation of deep networks," in *Proceedings of the 34th International Conference on Machine Learning - Volume 70*, ser. ICML'17. JMLR.org, 2017, p. 1126–1135.

[29] C. Li, S. Li, A. Zhang, Q. He, Z. Liao, and J. Hu, "Meta-learning for few-shot bearing fault diagnosis under complex working conditions," *Neurocomputing*, vol. 439, pp. 197–211, 2021. [Online]. Available: https://www.sciencedirect.com/science/article/pii/S0925231221001818

[30] O. Klejch, J. Fainberg, P. Bell, and S. Renals, "Speaker adaptive training using model agnostic meta-learning," in *2019 IEEE Automatic Speech Recognition and Understanding Workshop (ASRU)*, 2019, pp. 881–888.